Non-rigid registration of whole body planar images using mutual information.

Kurt De Moor*, Johan Nuyts, *Member, IEEE*, Patrick Dupont, Sigrid Stroobants, Paul Suetens, *Member, IEEE*, and Frederik Maes

***Abstract*— A non-rigid registration method is proposed that uses mutual information as a similarity measure, regularized by two penalties. One penalty behaves as if elastic rods are interconnecting neighboring pixels, and the other conserves topology by penalizing area changes. The method is applied to software phantoms to asses its stability and to demonstrate its potential in working with position dependent rigidity. The method is then applied to a whole body ^{99m}Tc-MDP bone scan with good visual result, and is also successfully applied in a patient specific dosimetry application.**

***Index Terms*— Mutual information, non-rigid registration.**

I. Introduction

Over the last years, nuclear medicine imaging is increasingly used in the staging and therapy response assessment of cancer patients. Typically, planar or tomographic whole body emission imaging is used for this purpose. This paper focuses on planar whole body imaging. With this technique, an image of the tracer distribution in the entire body of the patient is acquired. To decide if a treatment is effective or not, careful evaluation of all known tumor deposits before and after treatment is essential. To date, this correlation is done visually and especially if a lot of tumor deposits are present, this process is very time consuming. Subtraction of images before and after therapy would allow a faster evaluation of treatment response. However, this is only possible when the images taken at different time points are properly registered. For whole body scans this means we need non-rigid registration to compensate for differences in patient positioning on the scanner, but whereby the geometry of the lesions should not be altered. Another application where image registration would be useful is in dosimetry studies, where radiation exposure to different organs is calculated from measurements of the tracer uptake in these organs from a series of whole body scans acquired at multiple time points. The analysis of such image set would be greatly simplified if the images could be registered non-rigidly to compare radiation amounts.

Consequently, for this application, we need a non-rigid registration (NNR) algorithm, that can treat particular structures as (nearly) rigid (e.g. to avoid deformation of lesions). Moreover, the method should be able to register two images of the same patient, but with a very different tracer distribution (because we will study progression of disease and changes of tracer concentration over time).

In many registration methods, pixel based approaches are used, in which intensity similarity between corresponding pixels is taken as the driving force for registration. Examples of this are squared difference of intensities [12], correlation [9], [13], and mutual information [2]–[4], [8], [10], [11]. The latter technique has the advantage of being applicable to images with different intensity distributions. Mutual information is a concept from information theory that has been very successfully applied in rigid registration of medical images [2]–[4].

To register whole body scans however, non-rigid registration is needed. NRR involves finding a deformation field that maps each point in one image onto the corresponding point in the other image based on an appropriate image similarity measure. Regularization of the NRR problem is required to constrain the solution space to include only physically acceptable deformations and to make the problem well posed. One approach for NRR regularization is the representation of the deformation field using smooth basis functions such as splines [6]–[8]. Free-form NRR approaches, that use a non-parameterized expression for the deformation field, are generally more flexible than spline-based representations, but require appropriate smoothness constraints that are typically imposed by penalizing non-smooth deformations [5] or by modeling the deforming image as an elastic material [1] or viscous fluid [10], [11]. Linear elasticity has been used as a regularizer in [1], [11], [13]. Moreover current NRR algorithms typically impose spatially invariant regularization constraints that do not accommodate for local differences in rigidity in different image regions [8].

As argued above, we wish to extend current NRR strategies by incorporating flexible and spatially inhomogeneous models of object rigidity. In this paper we present a pixel based non-rigid registration method, based on penalized mutual information. The penalty consists of two terms. The first one models non-linear elastic behavior, the second one non-linear compressibility, ensuring preservation of topology. Weights, that can be attributed on a per pixel basis are introduced in the penalty function to locally tune the regularization behavior depending on tissue type.

To show the potential of the method, we applied it to software phantoms, a dosimetry study, and to a whole body bone scan. The whole body scan registration results were validated by visual inspection by physicians experienced in nuclear imaging.

This work was supported by F.W.O. grant G.0174.03.

* K. De Moor, J. Nuyts, P. Dupont and S. Stroobants are with the Department of Nuclear Medicine, Katholieke Universiteit Leuven, B-3000 Leuven, Belgium (e-mail:Kurt.Demoor@uz.kuleuven.ac.be).

P. Suetens and F. Maes are with the Laboratory for Medical Image Computing, Radiology-ESAT/PSI, Katholieke Universiteit Leuven, B-3000 Leuven, Belgium.

II. Theory

Non-rigid registration is about finding a transformation τ that maps every pixel j from image F, the floating image, to a pixel $q = \tau(j)$ from image R, called the reference image. To penalize inter pixel distance changes, a penalty function behaving as if elastic rods are interconnecting pixel pairs is chosen. This function is called the rod penalty C_{rod}. The rod penalty does not guarantee preservation of topology, therefore an area penalty C_{area} is also introduced. Non-rigid registration is treated as an optimization problem, the objective function to be optimized can be written as

$$O = I - \beta C_{rod} - \gamma C_{area}. \tag{1}$$

with I the mutual information, γ and β the relative weights of both penalties.

A. Mutual information

Mutual information $I(R, F)$ of two images is a measure of the amount of information one image F contains about the other image R, given the transformation τ has been applied to F. The mutual information can be expressed in terms of the joint and marginal histograms h_{rf}, h_r, and h_f with the following relationship :

$$I(R, F) = \sum_r \sum_f \left[\frac{h_{rf}}{N} . \ln \frac{N.h_{rf}}{h_r.h_f} \right] \tag{2}$$

To ensure a smoothly varying joint histogram as a function of the pixel coordinates, it is calculated with partial volume interpolation [3]. Note that the histogram is directly computed from the (deformed) coordinates and the original image, so no intermediate images have to be computed.

For optimization of an objective function, an iterative gradient ascent algorithm will be used, so the gradient of I in every pixel (x_j,y_j) has to be known [3] :

$$\frac{dI}{dx_j} = \sum_{r,f} \frac{dI}{dh_{rf}} \frac{dh_{rf}}{dx_j} = \sum_{r,f} \frac{1}{N} \left(\ln \frac{N h_{rf}}{h_r h_f} - I \right) \frac{dh_{rf}}{dx_j} \tag{3}$$

Here $\frac{dh_{rf}}{dx_j}$ is a histogram with the same dimensions as the joint histogram h_{rf}. The derivatives in the y_j direction can be calculated in the same way.

B. Penalty

Mutual information alone is not enough to non-rigidly register two images. A penalty function is needed that penalizes excessive deformations. Ideally this function should make it possible to take into account the underlying physical properties of the objects represented by these pixels, if such information is available.

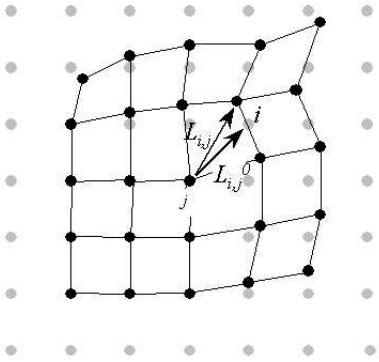

Fig. 1. Distances L^0 and L between pixel i and j in the undeformed and deformed image. w_ij is the weight we can give to an individual pixel to reflect the physical properties of the object the pixel represents.

1) Rod penalty: To penalize inter pixel distance changes, the rod penalty has been introduced. Figure 1 shows the pixel grid before and after deformation. As illustrated in this figure, the distance between pixel j and pixel i in the undeformed image is denoted $L^0_{i,j}$, and in the deformed image it is called $L_{i,j}$.

We want to optimize the objective function O, so part of the driving force toward an optimum is the derivative of the penalty C_{rod}. For this derivative, we propose the function

$$\frac{dC_{rod}}{dx_j} = \frac{1}{J} \sum_{i=1}^{8} w^r_{i,j} . \tan \left(\frac{\pi}{2.B} . X_{i,j} \right) . \frac{dX_{i,j}}{dx_j} \tag{4}$$

with

$$X_{i,j} = \frac{L_{i,j} - L^0_{i,j}}{L^0_{i,j}} \tag{5}$$

In this formula J is the number of pixels in the image, $w^r_{i,j}$ is the weight given to a pixel pair, r stands for rod. The weights can be used to incorporate anatomical knowledge. Assuming all pixels have been attributed to an anatomical class (e.g. bone, soft tissue ...), the weights $w^r_{i,j}$ can be adjusted to reflect the different physical properties of the classes. For a mixed pixel pair the highest weight is taken as the weight for the pixel pair. The sum over i takes into account the neighboring pixels of pixel j, that form a window around pixel j. We use the eight nearest neighbors of pixel j , but the algorithm allows other configurations if necessary.

Integrating the derivative of the penalty, the following function appears :

$$C_{rod} = -\frac{B}{\pi J} . \sum_{j=1}^{J} \sum_{i=1}^{8} w^r_{i,j} . L^0_{i,j} . \left[\ln(\cos(\frac{\pi}{2.B} . X_{i,j})) \right] \tag{6}$$

We divided C_{rod} by 2, because in the sum over j, every pixel pair $j - i$ is counted twice. In figure 2, the penalty function is shown for one pixel pair and weight one.

Figure 2 also shows the derivative of the cost with respect to $X_{i,j}$. For $X_{i,j} = B$, this force is infinite, which is undesirable. For numerical stability the tangent function is clipped for $X_{i,j} > B - \epsilon$ and $X_{i,j} < \epsilon - B$, with ϵ very small. B has

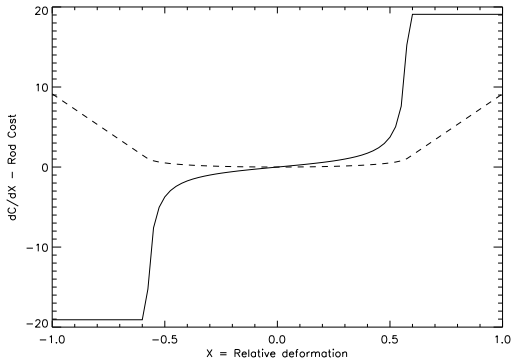

Fig. 2. Derivative of the rod cost in function of X. The function is clipped for $X = B - \epsilon$ and $X = -B + \epsilon$. In this figure, $B = 0.6$, $L^0 = 1.0$, and $\epsilon = 0.02$. Dashed line : Rod cost as a function of relative deformation X. Parameters : $B = 0.6$, $L^0 = 1.0$, and $\epsilon = 0.02$

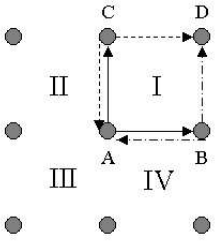

Fig. 3. Central point A and its eight neighbors. Vector product $\vec{AB} \times \vec{BC}$ is 2 times the surface of triangle $\widehat{ABC}$. The surroundings of point A are divided in 4 quadrants I to IV.

been chosen to be 0.6. We can consider B as the maximum allowable relative deformation. As shown in figure 2, the function slightly penalizes small deformations but strongly penalizes deformations close to B, and larger.

2) Area penalty: To preserve topology, the area penalty function has been designed. Consider a central pixel A and its 8 nearest neighbors, as shown in figure 3. Consider square I in the right upper corner. In this square 3 triangles can be drawn that change shape when the central pixel A moves, $\widehat{ABC}, \widehat{BAD}$ and $\widehat{CAD}$. Consider one of the triangles and take the natural logarithm of the area as the derivative of the cost. The area of the undeformed triangle equals one and yields a zero derivative. If the area shrinks, the derivative becomes negative and pushes the pixels apart.

The derivative of this second cost C_{area} is defined as :

$$\frac{dC_{area}}{dx_j} = \frac{1}{J} \sum_{i=1}^{4} \sum_{l=1}^{3} w^a_{i,l,j} . \ln(A_{i,l,j}) . \frac{dA_{i,l,j}}{dx_j} \qquad (7)$$

In this formula $A_{i,l,j}$ is the area that can be formed between pixel j (point A in figure 3), and the pixels in quadrant i, described as quadrant I to IV in figure 3, l denotes the 3 areas in every quadrant. The $w^a_{i,l,j}$ allow us to distinguish between classes of pixels. For every triangle, the highest value of the weights of the three corners is taken as $w^a_{i,l,j}$. The area of the 3 triangles $\widehat{ABC}, \widehat{BAD}, \widehat{CAD}$ are the vector products of vectors $\vec{AB} \times \vec{AC}$, $\vec{BA} \times \vec{BD}$, and $\vec{CA} \times \vec{CD}$, divided by two. This constant factor will be left out in the rest of the discussion.

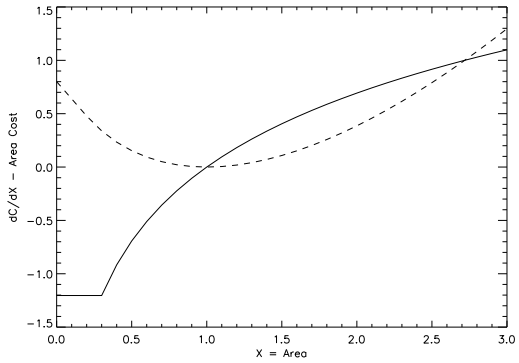

Fig. 4. Derivative of the area cost as a function of the area. The function clips for Area < 0.03 in this example. Area cost as a function of area in dashed.

Having defined this function the area cost function can be found by integration :

$$C_{area} = \frac{1}{3J} \sum_{j=1}^{J} \sum_{i=1}^{4} \sum_{l=1}^{3} w^a_{i,l,j} . (A_{i,l,j} \ln(A_{i,l,j}) - A_{i,l,j} + 1) \qquad (8)$$

where we divide by 3 because as we sum over j, every triangle appears in 3 (4 quadrant) constructions figure (3), so it is counted 3 times.

Figure 4 shows the derivative of the area cost as a function of the area for a single triangle. Also in this case the function is clipped to $\ln(\epsilon)$ when the area gets lower than a predefined value ϵ. Figure 4 also shows the area cost in function of the area.

C. Algorithm

The change in deformation field is calculated in every pixel as follows :

$$\Delta u = \text{Step.}(\nabla I - \beta . \nabla C_{rod} - \gamma . \nabla C_{area}) \qquad (9)$$

where Δu is the deformation added to the total deformation field by this iteration, ∇ denotes the gradient, and Step is a multiplication factor to speed up convergence. The Δu is added to the coordinates of the pixels of the floating image. Whatever the Δu calculated, its magnitude is limited to a maximum allowable value, $MaxDF$, which is currently set at 0.3 pixel. Too high a value for this parameter may prevent the algorithm from finding a realistic solution, too low a value slows down convergence.

This deformation calculation is repeated until Δu is smaller than a preset value, or until a number of iterations have been completed. The sum of all Δu for all iterations gives the total deformation field. To speed up convergence a step size is included in the calculation. The Step is initially set to one and is adjusted after every iteration (9). For that purpose, the angle θ between the current Δu and the Δu from the previous iteration is calculated. For θ going to zero, i.e. for consecutive displacements in the same direction, the step size is multiplied with a maximum multiplication factor $MaxMF = 10.0$.

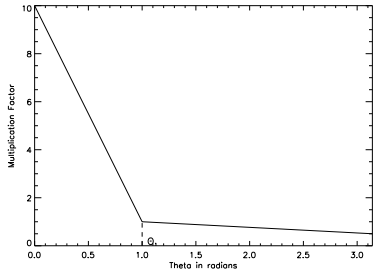

Fig. 5. Multiplication factor in function of the angle between the two deformation vectors.

TABLE I

PARAMETERS FOR THE CORE OF THE ALGORITHM.

	Symbol	Name	Value	Equation
Rod Cost	$w^r_{i,j}$	Weight air	0.008	6, 4
	$w^r_{i,j}$	Weight tissue	0.4	6, 4
	$w^r_{i,j}$	Weight bone	1.0	6, 4
	B	Max deformation	0.6	6, 4
Area Cost	$w^a_{i,j}$	Weight air	0.0001	8, 7
	$w^a_{i,j}$	Weight tissue	1.0	8, 7
	$w^a_{i,j}$	Weight bone	1.0	8, 7
General	Nbins	Number of bins	40	2, 3
	β	Weight rod cost	20	9
	γ	Weight area cost	2	9

For larger values of θ the step size is decreased or kept constant. Figure 5 shows the relationship between angle and multiplication factor. It is a piecewise linear curve, which equals 10 for $\theta = 0$, and 1 for $\theta = 1$ rad. In order to speed up convergence, and to allow for larger deformations, a multi resolution scheme is used, in which the images are subsampled in 8 steps starting with a sub sampling factor of 16 in each dimension. The procedure described in the previous paragraph is repeated for a next step up in resolution, decreasing the pixels size in each dimension by $\sqrt{2}$, until full resolution is reached.

Depending on the application 2 or 3 anatomical classes $w^r_{i,j}$'s were used in (4), and 2 or 3 $w^a_{i,j}$'s in (7). The tangent used for (4) has one parameter B (5). Tables I and II give an overview of all the parameters used.

The calculation of the resulting image is done by applying the deformation field to the floating image. In general a pixel from the floating image ends up between four neighbors in the resulting deformed image. The intensity of this pixel is then distributed with bilinear interpolation between the four neighbors. In this way no intensity is lost which is important in nuclear medicine imaging.

The number of bins we use to calculate the joint histogram is 40. All experiments we did with this value gave satisfactory results, so we did not find it necessary to evaluate this parameter further.

D. Application to whole body images

The procedure starts with a preprocessing step. The floating and reference image are clipped to remove extreme intensities

TABLE II

PARAMETERS FOR THE OPTIMIZATION.

Symbol	Name	Value
$MaxDF$	Max Δu	0.3
$MaxMF$	Max Step multiplication	10.0

TABLE III

PARAMETERS FOR THE PRE-PROCESSING STAGE.

Symbol	Name	Value
PreSmooth	f.w.h.m smoothing	2.5
Clip	Clipping input images	15.0

(e.g. due to tracer accumulation in the bladder) out of the image. We found that clipping to 15 times the mean of the image produces good results. It then proceeds with a Gaussian smoothing of reference and floating image, because nuclear medicine images are relatively noisy. No smoothing enhances the risk of getting trapped in a local maximum. Too much smoothing causes loss of detail. Here a Gaussian with a full width at half maximum of 2.5 pixels has been chosen (table III). The algorithm starts with a simple rigid registration, translating the floating image in such a way as to put its barycenter on the barycenter of the reference image. After this preprocessing step the non-rigid algorithm is applied.

III. EXPERIMENTS

A. Software phantom 1

A software phantom was made to study the behavior of the algorithm in case of position changes, head rotations, and leg rotations of a patient. The phantom is a combination of ellipses and rectangles representing the image of a patient, thereby only making use of two gray values. The image contains 128 x 512 pixels. The weight values for air and tissue from table I are used in formulas 4 and 7.

1) Leg rotation: To see if the algorithm can deal with large differences in patient position between scans, the phantom has been registered with different angles of leg rotation. The error between reference image and registered floating image has been calculated and plotted in function of rotation angle.

2) Parameter sensitivity: The error has been plotted as a function of β and γ, to asses the stability of the algorithm.

B. Software phantom 2

The second phantom has been designed to illustrate the use of non-uniform rigidity. The phantom contains two tissue classes, and a third class for air. In the floating image, the different tissue classes have different intensities, but they have identical intensities in the reference image. The images have 100 x 100 pixels.

C. Dosimetry application

For patient specific dosimetric calculations in radionuclide therapy, the patient is injected with a tracer amount of the radionuclide, and a series of planar whole body images

showing the bio-distribution of the tracer at different time points is acquired. To determine residence times in organs of interest, regions have to be drawn to delineate the organs on the whole body scans. Because the patient's position is somewhat different in every scan, the regions have to be moved in every scan. If the images have been properly aligned by registration, the delineation has to be performed only once. We applied our algorithm to a dosimetry study using ^{111} In (indium) labeled antibodies. After injection of the tracer , 5 whole body scans were taken at 15 min, 4 hours, 1 day, 3 days and 6 days. From these the third scan was taken as the reference image. The other four where then registered with respect to this third scan. The image dimensions are 256 x 1024 pixels. The weight values for air and tissue from table I are used in formulas 4 and 7.

D. Whole body ^{99m}Tc-MDP bone scans

To follow up lesions in cancer treatment, subtraction of images acquired at specific moments in time is useful, provided that the images are properly aligned. We give a typical example of non-rigid registration of two such scans. The images have 256 x 1024 pixels. In this application we use three weights, one for air, one for tissue, and one for bone pixels. The segmentation is done by smoothing, edge detection and thresholding. A barycenter calculation is used to do the rigid registration.

IV. Results

A. Software phantom 1

In figure 6 the 'head' and a 'leg' of the software phantom are both rotated in the floating image, with respect to the reference image. A good registration was obtained.

1) Leg rotation: Figure 7 shows the registration error in function of rotation angle. If we define S as the Gaussian smoothing (f.w.h.m. 2.5) of the difference image $I_R - I_F$, the registration error E_r is defined as :

$$E_r = \frac{\sqrt{\frac{\sum_{j=1}^{J} S_j^2}{J}}}{I_m} \tag{10}$$

with I_m the mean intensity of the reference image. The algorithm is able to register all angles shown in the graph.

2) Parameter sensitivity: Figure 8 and 9 show the registration error E_r as a function of β and γ, the relative weights of the rod penalty and the area penalty in relation to the mutual information.

B. Software phantom 2

Figure 10 shows the registration of 2 irregular structures. For this test we made the weights from formulas 4 and 7 much higher for the circular structure (a part called lesion) than the weights for the rest of the object (tissue). Table IV shows all the relevant data. The rest of the parameters are identical to the ones described in the algorithm section. The circular structure remains intact during deformation, whilst the tissue part deforms relatively easily. The intensity variations

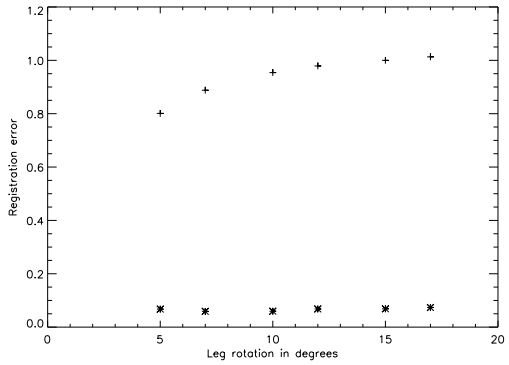

Fig. 7. Registration error in function of rotation angle. Upper part : after rigid registration, lower part after non-rigid registration.

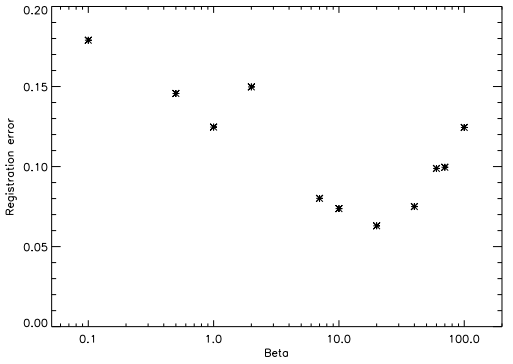

Fig. 8. Registration error in function of β. $E_r = 0.954$ after rigid registration, rotation angle of the leg is 10 degrees, $\gamma = 2.0$.

in the tissue part come from the way the deformed image is calculated as explained in the algorithm section. Because total activity is preserved, compressed tissue becomes darker.

In figure 11 the weights for lesion are much smaller than the weights for tissue. We can see a large deformation in the lesion part too, which shows the value of the weight concept.

C. Dosimetry images

The whole body bio-distribution images, used in patient specific dosimetry calculations, where registered with the same parameters as software phantom 1. Figure 12 shows a typical registration of an image with the third image out of a group

TABLE IV
PARAMETERS FOR SOFTWARE PHANTOM 2.

	Symbol	Name	Value	Equation
Rod Cost	$w^r_{i,j}$	Weight air	0.001	6, 4
	$w^r_{i,j}$	Weight tissue	0.2	6, 4
	$w^r_{i,j}$	Weight lesion high	10.0	6, 4
	$w^r_{i,j}$	Weight lesion low	0.1	6, 4
Area Cost	$w^a_{i,j}$	Weight air	0.0001	8, 7
	$w^a_{i,j}$	Weight tissue	1.0	8, 7
	$w^a_{i,j}$	Weight lesion high	10.0	8, 7
	$w^a_{i,j}$	Weight lesion low	0.1	8, 7

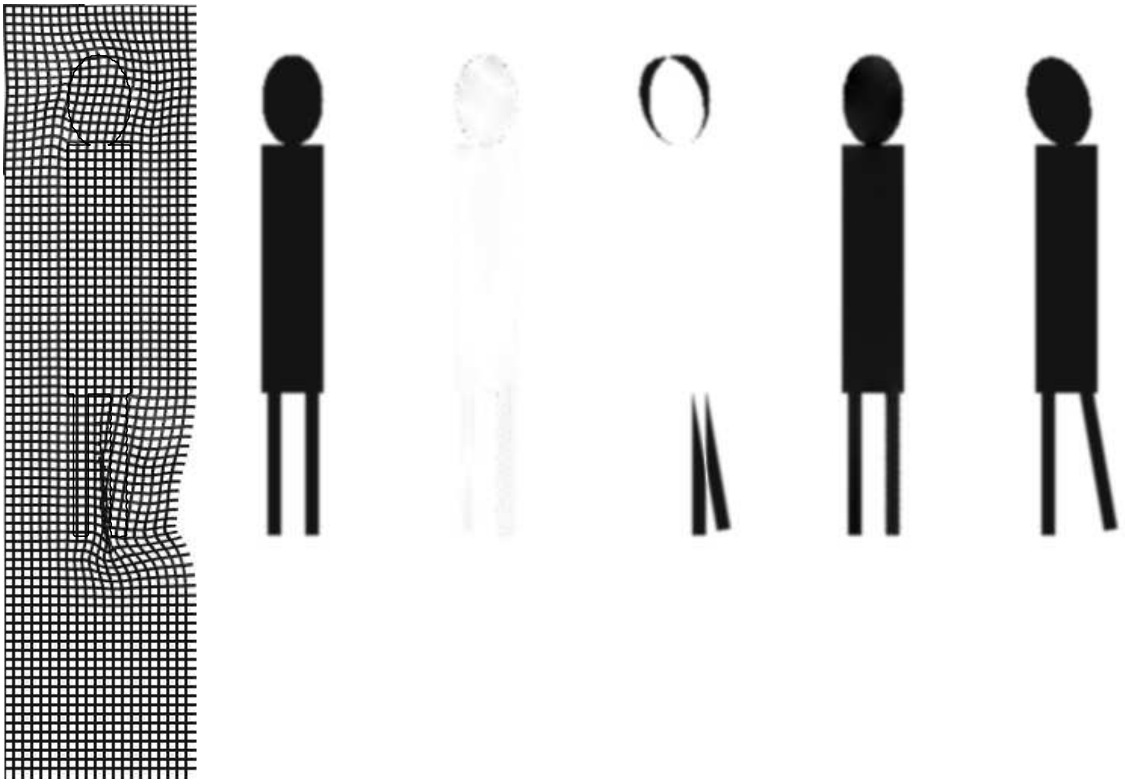

Fig. 6. Registration of phantom - from left to right deformation field, reference image, (absolute value of) subtraction of reference and deformed floating image, (absolute value of) subtraction of reference and floating image after rigid registration, deformed floating image, and floating image before deformation.

Fig. 10. Registration of irregular structure with circular 'lesion' - from left to right deformation field, reference image, (absolute value of) subtraction of reference and deformed floating image, deformed floating image, and floating image before deformation. The weights for the 'lesion' are high.

Fig. 11. Registration of irregular structure with circular 'lesion' - from left to right deformation field, reference image, (absolute value of) subtraction of reference and deformed floating image, deformed floating image, and floating image before deformation. The weights for the 'lesion' are low.

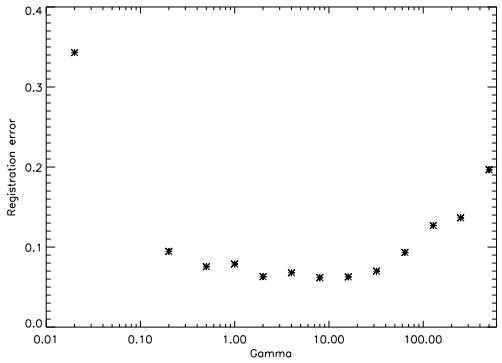

Fig. 9. Registration error in function of γ. $E_r = 0.954$ after rigid registration, rotation angle of the leg is 10 degree, $\beta = 20.0$.

of five taken as the reference image. All images were co-registered well according to visual assessment.

D. Whole body ^{99m}Tc-MDP bone scans

Whole body PET images were taken at two instances in time. The result of the registration is shown in figure 13.

V. Discussion

In this work, a non-rigid registration method is presented that makes use of mutual information as a similarity measure, regularized by an elastic type of rod penalty, and a topology preserving area penalty. Both penalties can be weighted on a per pixel basis to take underlying physical properties into account. A visual example of that is given in section 'Software phantom 2'.

In the pre-processing stage, a presmoothing and a clipping of the images is done, see table III. Too much smoothing causes loss of detail, no smoothing gives rise to many local optima, so a compromise of 2.5 pixels has been taken. Because nuclear images can have large intensity differences, e.g. between a hot lesion an cold background, a clipping has been applied that restricts the maximum intensity to 15 times the mean intensity value.

As shown in the experiments on 'Software phantom 1', the algorithm is relatively insensitive to β and γ, β having a range about 7, and γ having a range of about 100.

The optimization algorithm (parameters shown in table II) calculates Δu, proportional to the gradient of the objective function. This Δu is limited to 0.3 pixel, to allow the constraint to conserve topology, yet is big enough to allow for rapid convergence. A parameter affecting the convergence of the algorithm is the multiplication factor MF, with which 'Step' in formula 9 is multiplied. The principle of this factor is : when far from the maximum, Δu should be large to reach the maximum. When Δu starts to change direction, we are near the maximum, and therefore the multiplication factor should become smaller.

All the images shown and discussed in this article can be registered with the same parameters shown in tables, III, I and II.

Time to calculate a deformation field is a few minutes on a state of the art PC with Linux as the operating system.

Both penalty functions are normalized by the number of pixels in the image in formulas (4), (6), (7) and (8). This was done because the mutual information depends on the histogram, and is therefore insensitive to the number of pixels. In contrast, the penalty terms are summations over contributions per pixel. One might expect that the number of pixels should be adjusted at lower resolutions in the multi-resolution scheme. However, we found that performance was better if J was fixed at the number of pixels at full resolution in (4) - (8). At lower resolutions, the number of terms in the penalty decreases, but the value of the terms increases, because the deformations are calculated over larger distances. Currently, we have simply fixed the normalization, possibly a more sophisticated normalization could further improve the performance.

VI. Conclusions

A new algorithm for non-rigid registration was presented. It makes use of mutual information, regularized by a penalty function that allows for non-uniform rigidity, and that ensures that topology is preserved. The method is applied to software phantoms and clinical whole body scans with satisfactory results. In the future a 3D version of this method will be developed.

References

[1] R. K. Bajcsy and S. Kovacic, "Multi-resolution elastic matching," *Computer Vision, Graphics and Image Processing.*, vol 46(1), pp 1-21, 1989.

[2] A. Collignon, F. Maes, D. Delaere, D. Vandermeulen, P. Suetens and G. Marchal, "Automated multi-modality image registration based on information theory," *Proceedings of the XIVth International Conference on Information Processing in Medical Imaging, Computational Imaging and Vision*, vol. 3, pp. 263–274, Ile de Berder, France, June 1995. Kluwer Academic Press.

[3] F. Maes, A. Collignon, D. Vandermeulen, G. Marchal, and P. Suetens, "Multimodality image registration by maximization of mutual information," *IEEE transactions on medical imaging.*, vol 16(2), pp. 187–198, April 1997.

[4] P. Viola, and W. Wells, "Alignment by maximization of mutual information," *Int. journal of computer vision.*, vol 24(2), pp. 137–154, 1997.

[5] P. Hellier, C. Barillot, E. Memin, P. Perez, "Hierarchical estimation of a dense deformation field for 3-D robust registration," *IEEE Transactions on Medical Imaging.*, vol 20(5), pp. 388-402, 2001.

[6] C. Meyer, J. L. Boes, B. Kim, P. H. Bland, R. L. Wahl, K. R. Zasadny, P. V. Kison, K. Koral, and K. A. Frey, "Demonstration of accuracy and clinical versatility of mutual information for automatic multi-modality image fusion using affine and thin plate spline warped geo-metric deformations," *Medical Image Analysis.*, vol 1(3), pp. 195-206, 1997.

[7] D. Rueckert, L.I. Sonoda, C. Hayes, D.L.G. Hill, M.O. Leach, and D.J. Hawkes, "Nonrigid registration using free-form deformations : application to breast MR images," *IEEE transactions on medical imaging.*, vol 18(8), pp. 712–721, August 1999.

[8] T. Rohlfing, C.R. Maurer,Jr., D.A. Bluemke, and M.A. Jacobs, "Volume preserving nonrigid registration of MR breast images using free-form deformation with an incompressibility constraint," *IEEE transactions on medical imaging.*, vol 22(6), pp. 730–741, June 2003.

[9] J. Kim and J.A. Fessler, "Intensity-based image registration using robust correlation coefficients", *IEEE transactions on medical imaging.*, vol 23(11), pp. 1430–1444, November 2004.

[10] E. D'Agostino, F. Maes, D. Vandermeulen, and P. Suetens, "A viscous fluid model for multimodal non-rigid image registration using mutual information," *Medical image analysis.*, vol 7, pp. 565–575, 2003.

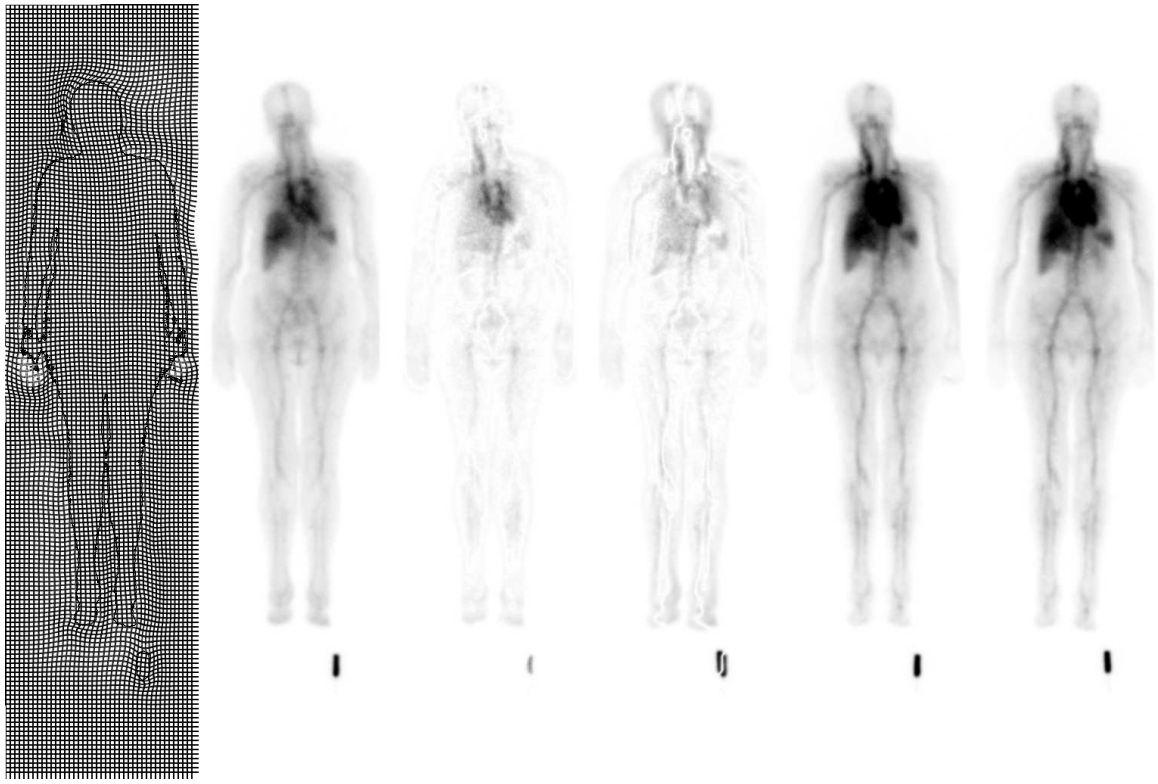

Fig. 12. Registration of whole body images for dosimetry calculations - from left to right deformation field, reference image (scan 3), (absolute value of) subtraction of reference and deformed floating image, (absolute value of) subtraction of reference and floating image after rigid registration, deformed floating image, and floating image before deformation (scan 5).

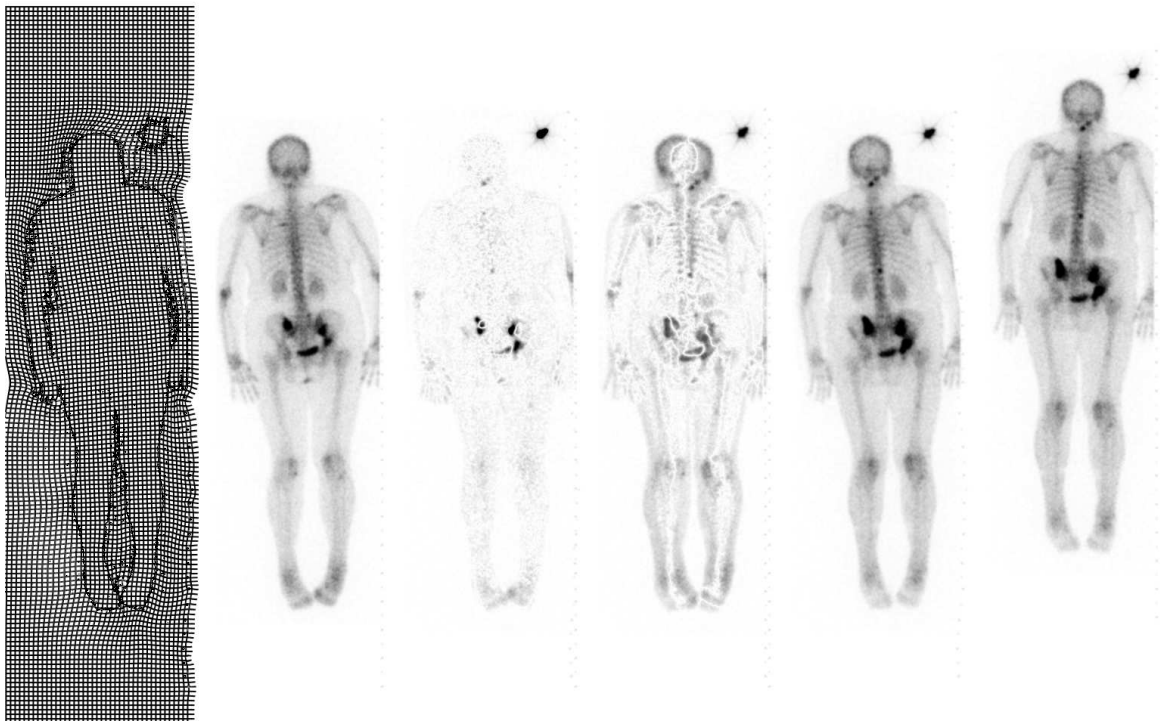

Fig. 13. Registration of Whole body ^{99m}Tc-MDP bone scans - from left to right deformation field, reference image, (absolute value of) subtraction of reference and deformed floating image, (absolute value of) subtraction of reference and floating image after rigid registration, deformed floating image, and floating image before deformation.

[11] G. Christensen, R. Rabbitt, and R. Miller, "Deformable templates using large deformation kinetics," *IEEE transactions on image processing.*, vol 5(10), pp. 1435-1447, 1996.

[12] J. Ashburner, J.L.R. Andersson, and K.J. Friston, "High-dimensional image registration using symmetric priors," *Neuroimage.*, 9, pp. 619-628, 1999.

[13] G. Hermosillo, C. Chef d'Hotel, and O. Faugeras, "A variational approach to multi-modal image matching," *Techn report 4117, INRIA-ROBOTVIS.*, Sophia Antipolis, France 2001.